https://doi.org/10.5194/egusphere-2025-1492
Preprint. Discussion started: 4 April 2025

Drivers of seasonal hydrography in Disko Bay, Greenland

Linda Latuta[1,2], Lars Henrik Smedsrud[1,2], Elin Darelius[1,2], Per Juel Hansen[3], and Josh K. Willis[4]

[1]Geophysical Institute, University of Bergen, Bergen, Norway
[2]Bjerknes Centre for Climate Research, Bergen, Norway
[3]Department of Biology, Marine Biological Station, University of Copenhagen, Helsingør, Denmark
[4]Jet Propulsion Laboratory, California Institute of Technology, Pasadena, CA, USA

Correspondence: Linda Latuta (linda.latuta@uib.no)

Abstract. This study investigates the seasonal dynamics of Disko Bay in West Greenland. On the eastern side, the hydrography in the bay is driven by ice-ocean interactions and exchange with Ilulissat Icefjord, and on the western side, it exchanges waters with Baffin Bay. Since the mid-1990s, this region has experienced significant changes, including rapid ocean warming, sea-ice decline, and the retreat of Greenland's fastest-flowing marine-terminating glacier. Although West Greenland Irminger Water (WGIW) is known to be a heat source behind many of these changes, it has remained unclear when and how these dense warm waters flow into Disko Bay. We present a 2-year hydrographic record of observations within Disko Bay, determining the key hydrographic seasonality and the processes that drive it. Dense water renewal occurs repeatedly each spring when WGIW crosses the sill between Baffin Bay and Disko Bay. This spring renewal leads to the highest observed temperature and densest waters at depth, which rise high enough in the water column to reach the Ilulissat Icefjord sill. Additionally, we show that renewal may occur in late autumn and winter in the presence of upwelling-favourable winds along the West Greenland shelf. Following the renewal-driven season in spring, the summer and autumn are characterised by a deep-reaching fresh signal that extends over the upper 150 m across large areas of Disko Bay. Spatial analysis reveals an advective path that transports this fresh signal westward from the vicinity of Ilulissat Icefjord, along the northern periphery of the bay. Additional seasonal influence comes from along-isopycnal warming below this fresh layer, which is observed throughout autumn.

1 Introduction

Disko Bay (Qeqertarsuup Tunua) is the largest open-water embayment in West Greenland (Fig. 1). Bordered by Baffin Bay to the west and numerous glacial fjords to the east, its hydrography is shaped by a complex interplay of regional water mass exchanges, local oceanographic processes, and ice-ocean interactions. Since the late 1960s, oceanographic studies in Disko Bay have provided valuable insights into its hydrography and circulation patterns (Petersen, 1964; Muench, 1971; Andersen, 1981a). Subsequent research explored seasonality and the associated ecosystem functioning (Andersen, 1981b; Nielsen TG and Hansen B, 1995), while more recent studies have documented significant changes in the oceanographic conditions over the past decades (Hansen et al., 2012; Myers and Ribergaard, 2013). A notable transition occurred in the mid-1990s when the increased presence of warm Atlantic-origin waters marked the transition from a cold to a warm regime in Disko Bay (Holland et al., 2008; Hansen et al., 2012). This warming was particularly evident at 200-250 m depth, corresponding to the depth

https://doi.org/10.5194/egusphere-2025-1492
Preprint. Discussion started: 4 April 2025

at which warm waters can enter Ilulissat Icefjord. By the late 1990s, temperatures at this depth had risen from ∼1.5°C to ∼2-2.5°C, eventually surpassing 3°C in the early 2000s (Hansen et al., 2012; Khazendar et al., 2019; Joughin et al., 2020). This warming has been linked to the disintegration of the floating ice tongue and the increased melting of Sermeq Kujalleq (Jakobshavn Glacier), Greenland's fastest flowing marine-terminating glacier, located within Ilulissat Icefjord (Holland et al., 2008; Motyka et al., 2011; Khazendar et al., 2019). Sermeq Kujalleq's response to oceanic forcing and the exchange of water masses between Disko Bay and Ilulissat Icefjord (Gladish et al., 2015a) highlights the importance of continued monitoring to better understand the oceanographic processes governing these interactions.

Despite extensive long-term observations, most available data were collected from April to September, leaving gaps in our understanding of seasonal oceanographic variability. Winter sea-ice cover and harsh conditions have historically limited data collection, making it difficult to obtain sufficient temporal and spatial data coverage to determine the seasonality of water masses in Disko Bay. In particular, the seasonality of warm subsurface waters remains poorly understood. While it has been hypothesised that deep warm waters in Disko Bay renew during winter/spring (Gladish et al., 2015a), the lack of winter and early spring observations has left this process largely unexplored. Moreover, Disko Bay is a recipient of glacially modified waters exported from Ilulissat Icefjord. While detailed studies have examined these waters near the fjord (Beaird et al., 2017; Hopwood et al., 2025), their fate across a broader spatial and seasonal scale in the bay remains unclear.

This study presents oceanographic observations spanning two annual cycles from June 2022 to October 2024, supplemented by a regional survey conducted in the summer of 2018. These observations provide new insights into the seasonal processes shaping Disko Bay's hydrography and how its waters respond to external forcing on seasonal timescales. We analyse these observations to shed light on the following three questions: 1) How does the hydrography within the bay evolve throughout the year? 2) What spatial patterns can be observed inside the bay? 3) What local or external processes drive the observed seasonal and spatial variability?

2 Regional setting

The regional circulation in Baffin Bay consists of three major currents: the northward-flowing West Greenland Current (WGC) and West Greenland Coastal Current (WGCC), as well as the southward-flowing Baffin Island Current (BIC) (Fig. 1a). The WGC carries warm and saline subsurface waters of North Atlantic origin along the continental shelfbreak of West Greenland (Pacini et al., 2020; Huang et al., 2024). Most of these warm waters divert west and south in the northern Labrador Sea, but some continue north past the Davis Strait into Baffin Bay. Upon crossing the Davis Strait, warm waters subduct below fresher and colder Polar-origin waters and continue propagating north as a bottom intensified current along the continental slope (Huang et al., 2024). Despite the heat loss caused by mixing with the polar water above, the subsurface warm waters remain the predominant heat source and cause of accelerated melt of many of the marine-terminating glaciers along West Greenland (Holland et al., 2008; Straneo et al., 2012; Khazendar et al., 2019; Joughin et al., 2020).

Inshore of the WGC, the WGCC carries the freshest waters along the Greenland Coast, consisting of meltwaters from the Arctic Ocean and Greenland Ice Sheet (Fig. 1a) (Foukal and Pickart, 2023). These waters travel south along the East

https://doi.org/10.5194/egusphere-2025-1492
Preprint. Discussion started: 4 April 2025

Greenland coast, around Cape Farewell, and then propagate northward towards the Davis Strait (Gou et al., 2022; Foukal and Pickart, 2023). North of the Davis Strait, the location and fate of WGCC are less clear due to meandering and spatial variability that is hard to resolve (Huang et al., 2024).

Topography modulates the exchange of waters between Baffin Bay and Disko Bay. A 300-900 m deep trough called Egedesminde Dyb (ED) cuts across the continental shelf, allowing dense and warm waters from the shelf break to enter Disko Bay (Fig. 1a). However, the passage of these warm waters is obstructed by Egedesminde Dyb Sill (EDS), which extends to 300 m depth and creates a barrier similar to a fjord sill (Fig. 1b) (Gladish et al., 2015a). We view EDS as the western boundary of Disko Bay and the approximate delineation of the Disko Bay - Baffin Bay boundary. The coast defines the eastern and southern boundaries. In the east, Disko Bay exchanges waters with Ilulissat Icefjord (750-800 m deep), where a shallow sill (deepest point of 245 m), also referred to as the Iceberg Bank, separates the two (Gladish et al., 2015b; Morlighem et al., 2022). Disko Island is located in the north of the bay, separated from the mainland to the east by Vaigat Strait. Shallow bathymetry (245 m) separates Disko Bay and Vaigat Strait (Andersen, 1981a; Morlighem et al., 2022). Thus, Disko Bay is confined by shallow and complex bathymetry and its deepest central area (300-500 m) is isolated from direct water mass exchanges.

Previous studies indicate generally cyclonic circulation within the bay (Andersen, 1981a; Sloth and Buch, 1984), following the bathymetry contours, with northward flow past Ilulissat Icefjord (Beaird et al., 2017), and outflow out of the bay via Vaigat Strait and along the south of Disko Island (Andersen, 1981a; Hansen et al., 2012).

3 Data and methods

3.1 Oceanographic observations

We use a combination of new observations from two drifting profilers and a hydrographic field campaign, together with existing data from the monitoring station in Disko Bay, to construct a hydrographic time series for 2022-2024. Table 1 gives an overview of all hydrographic profiles that make up the 2022-2024 time series, and profile locations are shown in Fig. 1b. Additionally, we utilise profiles from two hydrographic surveys in 2018 for a spatial analysis. Below, we describe each dataset.

3.1.1 Monitoring station

We use hydrographic data from the Greenland Ecosystem Monitoring Programme (GEM), which conducts observations on board RV $Porsild$ at an oceanographic monitoring station in northwestern Disko Bay (Table 1, Fig. 1b, Greenland Ecosystem Monitoring (2025a)). We obtained all available processed observations from GEM monitoring station between June 2022 and November 2023, which were taken with Sea-Bird SBE 19plus instrument with nominal accuracies of $\pm$ 0.005°C for temperature, $\pm$ 0.005 mS cm^{-1} for conductivity and 0.1% of full-scale range for pressure.

In addition, we conducted weekly measurements at the monitoring station from RV $Porsild$ throughout the autumn of 2023 (Table 1, Fig. 1b). We aimed to supplement the GEM profiles over 2023 with higher temporal resolution, targeting the undersampled autumn period. We measured temperature, conductivity, and pressure using the same Sea-Bird SBE 19plus

https://doi.org/10.5194/egusphere-2025-1492
Preprint. Discussion started: 4 April 2025

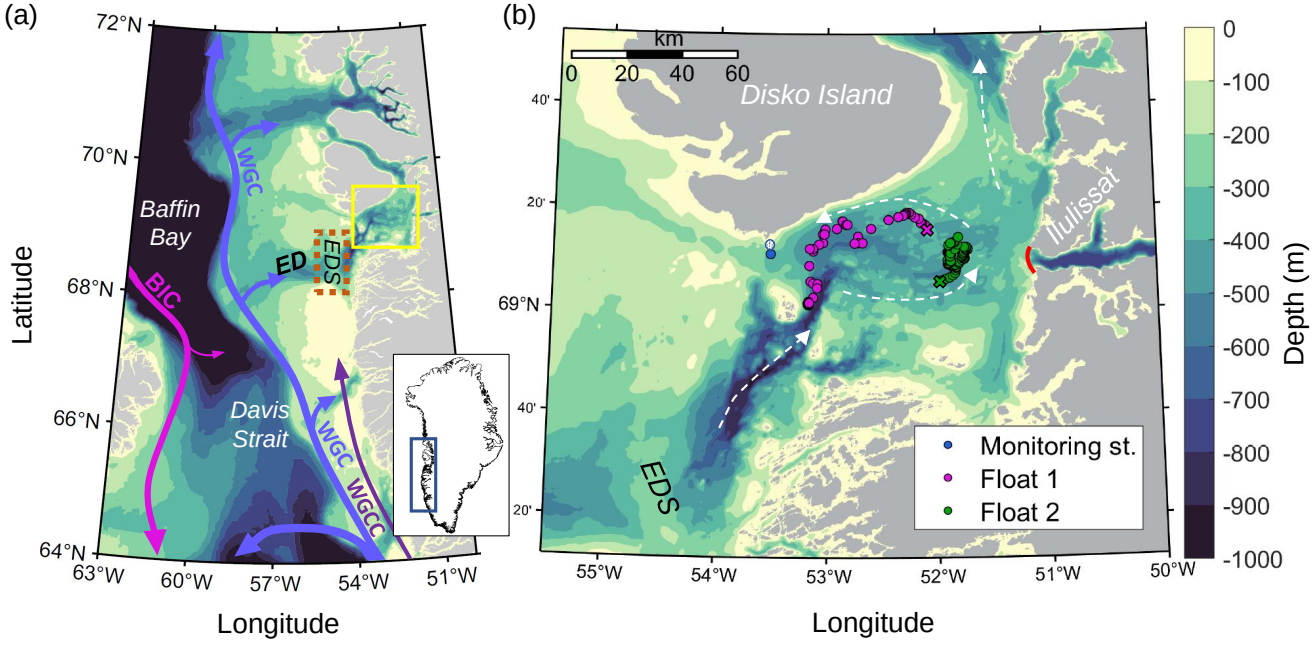

Figure 1. (a) Baffin Bay and West Greenland bathymetry, overlaid with north-flowing West Greenland Current (WGC, blue), West Greenland Coastal Current (WGCC, purple) and south-flowing Baffin Island Current (BIC, pink). The Egedesminde Dyb trough (ED) cuts across the continental shelf, entering Disko Bay (yellow box). The shallow Egedesminde Dyb Sill (EDS) is where we analyse wind forcing with ERA5 reanalysis data (orange dotted box). (b) Disko Bay bathymetry, Ilulissat Icefjord Sill (red line) and general circulation (white arrows, adapted from Hansen et al. (2012)). Location of oceanographic observations: monitoring station (blue circle), profile taken from landfast sea-ice (white circle with blue outline), Float 1 (Aug 2022 - June 2023, pink circles) and Float 2 (Aug 2023-Oct 2024, green circles). Each float's first profile is marked with a cross. Bathymetric data are from BedMachine Version 5 dataset (Morlighem et al., 2022).

instrument as used in GEM. We processed the raw data using Sea-Bird Scientific's SBE Data Processing (v7.26.7) application and standard quality control, correction, and processing steps. Similarly, one profile was taken in March 2023 at the landfast sea-ice edge (Table 1, Fig. 1b), 2.8km landward from the monitoring station.

We combined our field observations from this monitoring station (including the profile taken from sea ice) and the GEM data to construct a spatially fixed time series, which we refer to as "Monitoring station". We use TEOS10 Gibbs-Sea Water Oceanographic Toolbox (McDougall and Barker, 2011) to convert conductivity to Absolute Salinity (S_A), temperature to Conservative Temperature (CT), and pressure to depth. Throughout this manuscript, we refer to Absolute Salinity and Conservative Temperature as salinity and temperature, respectively. Hereafter, we refer to potential density anomaly with a reference pressure of 0 dbar (σ_0) as density.

https://doi.org/10.5194/egusphere-2025-1492
Preprint. Discussion started: 4 April 2025

3.1.2 Profiling float data

We use temperature and salinity profiles from an Air-Launched Autonomous Micro Observer (Alamo) float (ID: F9313), deployed in Disko Bay as part of the NASA Oceans Melting Greenland (OMG) Mission (Table 1,Oceans Melting Greenland (2022)). The float followed the general circulation (Fig. 1b). Between the 6th of February and the 4th of April, 2023, the float was profiling underneath the sea ice, and no information about the float's position during that period is available. However, between the acquisitions with known positions, the float's position changed only by 3.1km. The float data was quality controlled following the recommended procedures in Wong et al. (2024). Hereafter, we refer to this profiling float as Float 1.

Additional profiles were retrieved by an Apex float (WMO ID: 6990591) (Argo, 2024), deployed in Disko Bay in August 2023 as part of the Greenland Ocean Observations (GOO) project (Table 1, Fig. 1b). The data is Real-time and quality-controlled. We use only the data with a "good data" quality flag and follow up with the same quality control checks and processing as for Float 1.

Both Float 1 and 2 were fitted with RBR sensors with nominal accuracies of $\pm$ 0.002°C for temperature, $\pm$ 0.003 mS cm^{-1} for conductivity and $\pm$ 1 dbar for pressure. Salinity obtained from both floats was compared against CTD observations to check for possible salinity sensor drift, which was estimated to be less than 0.02 PSU over the span of operation of either float.

3.1.3 Hydrographic surveys in 2018

We utilised data from two hydrographic surveys conducted in the summer of 2018 (Table 1, Fig. 7a), which we used to analyse the spatial variability in the bay during the summer months. These near-synoptic cruises were conducted as part of the GEM programme (Greenland Ecosystem Monitoring, 2025b) covering most of Disko Bay's deep basin and using the same instrument as for the monitoring station observations. The first cruise was conducted on the 27-30th of May (Fig. 7a), and the second one was from the 30th of August to the 1st of September 2018 (Fig. 7a).

3.2 Atmospheric and sea-ice data

To estimate atmospheric forcing on local ocean variability in Disko Bay and across the shelf region, we used the European Centre for Medium-Range Weather Forecasts ERA5 reanalysis product (Hersbach et al., 2023). The product has 0.25° spatial and hourly temporal resolution. We obtain sea-ice concentration and 10-m u and v wind components over a region covering EDS (Fig1a).

For the sea-ice concentration inside Disko Bay, we use sea-ice concentration (SIC) from merged MODIS-AMSR2 satellite product (Ludwig et al., 2020). Daily SIC with 1km resolution was downloaded for the Disko Bay region (68°42'N - 69°31'N, 51°24'W - 53°W) and averaged spatially to obtain time series of weekly mean sea-ice concentration.

https://doi.org/10.5194/egusphere-2025-1492
Preprint. Discussion started: 4 April 2025

Table 1. Overview of analysed hydrographic observations.

Name	Period	Location	Profiles	Sampling frequency	Operated by
Monitoring station	Jun 2022 to Nov 2023	69°10'N 53°31'W	16	monthly	GEM
Monitoring station	Aug to Nov 2023	69°10'N 53°31'W	6	weekly	fieldwork
Monitoring station (from sea-ice)	Mar 2023	69°12'N 53°31'W	1	once	fieldwork
Float 1	Aug 2022 to Jun 2023	Trajectory Fig. 1b	63	5-day interval from 22 Sep 2022	NASA OMG
Float 2	Aug 2023 to Oct 2024	Trajectory Fig. 1b	74	5-day interval from 17 Oct 2023	GOO
Hydrographic surveys	May, Aug 2018	Marked in Fig. 7a	37, 20	near-synoptic	GEM

3.3 Methods

3.3.1 Determination of the mixed-layer depth

Based on the calculated density, we determine mixed-layer depth (MLD) for each hydrographic profile. We find MLD using the two-step method outlined in Semper et al. (2024). First, the preliminary MLD is computed from density profiles. We compute the normalised sum-of-squared errors of densities from the surface down to all possible depth combinations. When a sharp increase in normalised sum-of-squared errors occurs, we detect the depth of the mixed-layer (MLD). We then inspect each profile and confirm that temperature, salinity, and density between the surface and calculated MLD fall within one standard deviation envelope (Pickart et al., 2002; Semper et al., 2024).

https://doi.org/10.5194/egusphere-2025-1492
Preprint. Discussion started: 4 April 2025

3.3.2 Water mass definitions

Two water masses broadly describe the vertical structure of Disko Bay: a relatively cool and fresh layer of Arctic origin (blue shading in Fig. 2b), which overlays warmer and more saline waters of Atlantic origin (red shading in Fig. 2b).

The Arctic- and the Atlantic-origin waters found in Baffin Bay and the vicinity of Disko Bay have been referred to by several names. The Atlantic-origin waters are often called Modified Irminger Water (Gladish et al., 2015a), Subpolar Mode Water (Rysgaard et al., 2020), Atlantic Water (Beaird et al., 2017) and West Greenland Irminger Water (Curry et al., 2014; Carroll et al., 2018; Huang et al., 2024). These definitions broadly overlap in the properties they describe, and all point to the subtropical Atlantic origin of the warmest waters found along West Greenland. We refer to this water mass as West Greenland Irminger Water (WGIW, Fig. 2a).

Similarly, the cool and fresh waters found on the West Greenland shelf have also been termed differently, referring to a different origin of these waters or their formation process. For example, West Greenland Shelf Water and Arctic Water (Curry et al., 2014; Carroll et al., 2018), Baffin Bay Polar Water and Coastal Water (Rysgaard et al., 2020), cold Polar Water and warm Polar Water (Huang et al., 2024). Most studies looked at near-synoptic data covering large areas of Baffin Bay to delineate these water masses. In this study, we do not differentiate between the origins of the Arctic-origin water inside Disko Bay. Instead, we focus on the seasonal transformations within the present cool and fresh water mass over a given year, and thus, we use the more general term Polar Water (PW, Fig. 2a), similar to Myers and Ribergaard (2013), Beaird et al. (2017) and Muilwijk et al. (2022).

Hence, we maintain a simple two-layer structure definition for our study: West Greenland Irminger Water (WGIW) and Polar Water (PW). We define WGIW in Disko Bay as waters with a density $\sigma_0 > 27.2$ kg m^{-3}(thick isopycnal line in Fig. 2), matching the properties presented by Curry et al. (2014) and those found to be important in the exchange between Disko Bay and Ilulissat Icefjord basin (Gladish et al., 2015a, b). The lighter PW has density $\sigma_0 < 27.2$ kg m^{-3}. Through this paper, we also refer to the surface layer, which is defined as the extent of the mixed layer found within PW.

Freshwater fluxes are a vital driver of spatial and seasonal variability in Disko Bay, considering the significant glacial influence in the region (Mernild et al., 2015; Enderlin et al., 2016; Beaird et al., 2017). The major glacial freshwater input comes from Ilulissat Icefjord, where freshwater fluxes can be partitioned into liquid and solid components (Mernild et al., 2015; Enderlin et al., 2016; Beaird et al., 2017). A striking feature of the Ilulissat Icefjord is its abundance of icebergs. Icebergs are responsible for most of the freshwater flux at the terminus of Sermeq Kujalleq (Gladish et al., 2015b; Enderlin et al., 2016), representing the solid freshwater component. Icebergs drift and melt as they cross the fjord and the sill into the bay. Thus, when melting, icebergs transition from solid to liquid freshwater flux.

The liquid freshwater fluxes are runoff and Submarine Melt Water (SMW, Fig. 2a). SMW is formed when marine-terminating glaciers (or icebergs) melt directly from the heat supplied by the ocean (Θ = -90°C, S_A = 0 g kg^{-1}) (Gade, 1979). Runoff is the surface melt of glaciers and snow, which commonly enters the fjord at depth since runoff percolates into glacial crevasses and drainage channels, entering the fjord at the glacier's base (Straneo and Cenedese, 2015). Runoff that enters the fjord this way is termed Subglacial Discharge (SGD, Θ = 0°C, S_A = 0 g kg^{-1}, Fig. 2a). Together, SGD and SMW drive convective upwelling

https://doi.org/10.5194/egusphere-2025-1492
Preprint. Discussion started: 4 April 2025

inside the fjord, mixing and entraining the ambient waters at depth and bringing them upwards in the fjord's water column. The final product, Glacially Modified Water (GMW - mixture of ambient waters, SGD, and SMW, Fig. 2a) equilibrates at the level of neutral buoyancy within the fjord (Muilwijk et al., 2022).

3.3.3 Wind stress and Ekman pumping calculation

Zonal wind stress (τ_x) and meridional wind stress (τ_y) are computed for each grid point of the ERA5 fields of u_{10} and v_{10} wind speed components. We consider the impact of sea ice on wind stress by incorporating ERA5 sea-ice concentration (A) to obtain the 10-m neutral drag coefficient C_{dn10} following Lüpkes and Birnbaum (2005) parametrisation

$$C_{dn10} = (1 - A)C_{d,w} + AC_{d,i} + C_{d,f} \tag{1}$$

where $C_{d,i}$ and $C_{d,w}$ are the skin drag coefficients over sea ice and open water, for which we used $C_{d,i} = 1.89 \cdot 10^{-}3$ and $C_{d,w} = 1.25 \cdot 10^{-}3$ as in Lüpkes and Birnbaum (2005). The form drag coefficient, $C_{d,f}$, is estimated as

$$C_{d,f} = 0.34A^2 \frac{(1 - A)^{0.8} + 0.5(1 - 0.5A)^2}{\alpha_r + 90A} \tag{2}$$

where α_r is the aspect ratio D_i/h_f of mean floe length (D_i) to mean freeboard (h_f), which can also be estimated from A as

$$h_f = 0.49[1.0 - exp(-5.9A)] \tag{3}$$

$$D_i = 31h_f/(1 - A) \tag{4}$$

The Ekman pumping velocity (W_{Ek}) is then calculated with the curl of the surface wind stress as

$$W_{Ek} = \frac{1}{\rho_0 f_0}\left(\frac{\partial \tau_y}{\partial x} - \frac{\partial \tau_x}{\partial y}\right) \tag{5}$$

where f_0 is Coriolis parameter calculated for each grid cell, ρ_0= 1027.0 kg m^{-3} is a reference density and ∂x and ∂y are grid width and height.

4 Results

4.1 Water masses

The principal water masses can be identified from Fig. 2a-b, which present all the observations used in this study. At the surface, within the mixed layer, PW temperature ranges from in situ freezing temperature to a maximum of ~ 8°C during

https://doi.org/10.5194/egusphere-2025-1492
Preprint. Discussion started: 4 April 2025

summer (Fig. 2a,b). Mixing with various freshwater sources lowers the surface salinity to $\sim$ 31 g kg^{-1} in summer. During the winter, sea-ice formation and brine rejection increase the surface salinity to a range of 33-33.4 g kg^{-1}. The PW below the mixed layer exhibits a similarly broad temperature range, spanning from ~ 0 to 4°C. It reaches the coldest temperatures in winter alongside mixed-layer deepening and cooling. Once the sea ice melts, the surface waters re-stratify and warm due to solar insulation. The PW below then forms a characteristic temperature minimum in the water column (seen in the average profile in Fig. 2b). The WGIW, characterised by $\sigma_0 > 27.2$ kg m^{-3}, ranges from $2-4°C$ and reaches ~ 34.6 g kg^{-1} in salinity, showing less variability compared to PW (Fig. 2a,b).

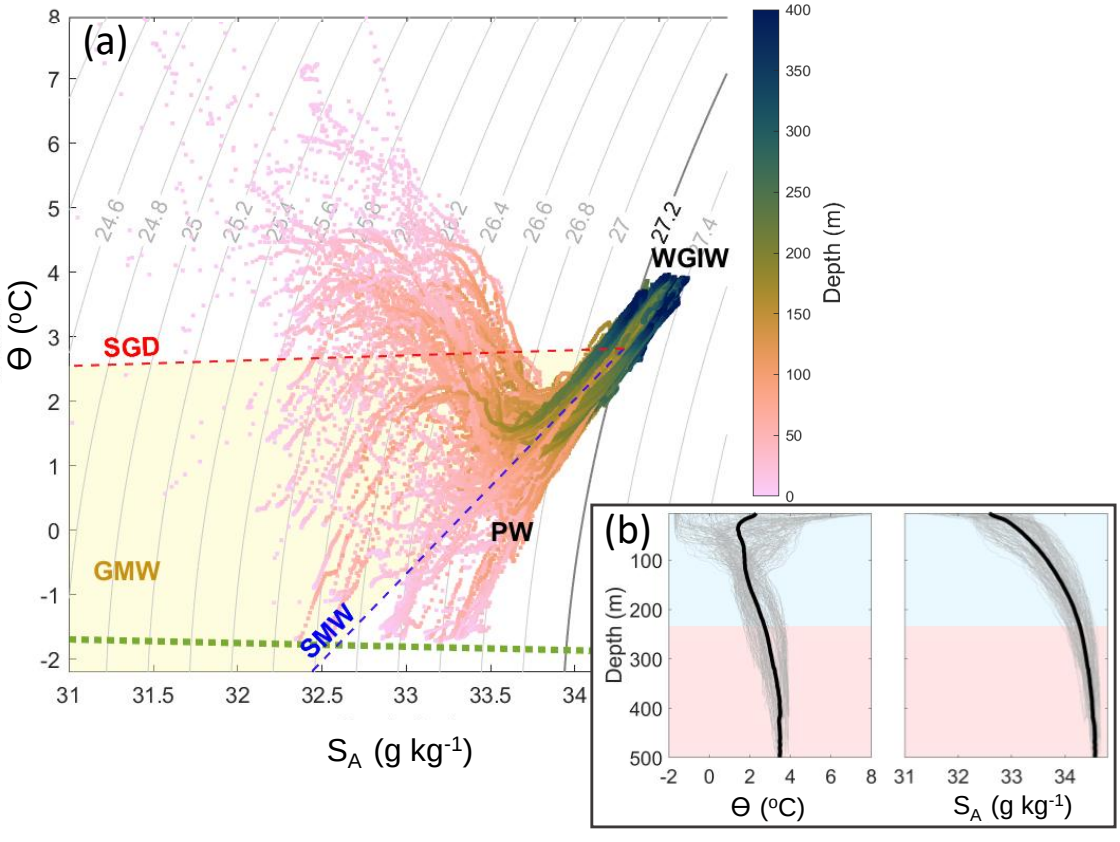

Figure 2. (a) Temperature (Θ) - Salinity (S_A) diagram for all observations between June 2022 and October 2024 (dots coloured by depth). Grey contours show isopycnals at 0.2 kg m^{-3} intervals referenced to surface pressure. The 27.2 kg m^{-3} isopycnal is marked (thick grey line) as it delineates West Greenland Irminger Water (WGIW) and Polar Water (PW). Dashed lines show mixing lines between the mean WGIW properties and Subglacial Discharge (SGD, Red) and Submarine Meltwater (SMW, Blue). Yellow shading between these two mixing lines marks the typical properties of glacially modified waters (GMW). The dotted green line marks the surface freezing point. (b) Temperature and salinity profiles from Disko Bay (thin grey lines), overlaid by a mean profile (thick black lines). Red and blue shadings mark WGIW and PW, respectively, with the boundary defined by the density of the mean profile.

https://doi.org/10.5194/egusphere-2025-1492
Preprint. Discussion started: 4 April 2025

The observations are also presented as time series in Fig. 3. The observations collected at the monitoring station closely match those obtained by the floats during the periods of overlap, confirming the reliability of our approach in combining these sources. Additionally, there is a consistent temporal pattern in the hydrographic development across both years and all observational platforms, suggesting the presence of a seasonal cycle that we will examine in further detail.

4.2 Surface mixed layer modifications

Both MLD, mixed-layer salinity, and mixed-layer temperature have a clear annual cycle that follows a consistent development over the two years (Fig. 4).

Mixed-layer temperature is at the in situ freezing point, and salinity is at the annual maximum value of 33.4 g kg^{-1} when the bay is sea-ice covered (Fig. 4b,c). When sea ice starts to melt in late April, mixed-layer temperature increases, and we see a drop in salinity. This onset of sea-ice melt in late April is consistent for both 2023 and 2024 and agrees well with satellite-derived SIC, which then drops below 10%. Sea-ice melt reduces the MLD, and this shallow layer (<20 m) is warmed by solar insulation (Fig. 4a,b). As summer progresses, MLD remains small due to increasing surface freshwater input, which lowers salinity by $\sim$2 g kg^{-1}. In August/September, mixed-layer salinity is at its lowest (31-31.4 g kg^{-1}) and the temperature at its highest value (8-10°C) (Fig. 4b,c). Over autumn, the mixed layer cools and deepens, together with a gradual increase in salinity. Eventually, the maximum MLD is reached during winter (73m in winter 2022-2023, 48m in 2023-2024), with temperature again reaching the in situ freezing point (Fig. 4a,b). This then allows sea-ice formation and a further increase in salinity through brine rejection (Fig. 4c).

4.3 Changes in the Polar Water

4.3.1 Temporal variability

From the time series in Fig. 3 we see that at the start of each summer, near-surface salinities are reduced in conjunction with mixed-layer freshening. This creates a stratified layer with a core that is bound approximately by $\sigma_0 = 26.5$ kg m^{-3} isopycnal (Fig. 3e,f). We follow the seasonal development of this surface-intensified layer by plotting the two annual cycles of mean salinity in the upper 150 m (Fig. 5a), capturing the depth range that this stratified fresh layer (approximated by $\sigma_0 =$ 26.5 kg m^{-3} isopycnal) extends over (Fig. 5b). In both years, the mean upper 150 m salinity begins to decrease in May-June (Fig. 5a) alongside a gradual deepening of the stratified layer down to 50m by the end of summer (Fig. 5b). Later in the year, the stratified layer deepens rapidly down to $>$ 100 m at the start of autumn, with salinity continuing to decrease throughout the autumn (Fig. 5a,b). This autumn decline in upper 150 m salinity continues after the mixed-layer salinities reached their minimum in late August. Overall, the PW salinity over the upper 150 m shows an annual cycle with an amplitude of $\sim$0.8 g kg^{-1}.

We investigate PW seasonality in more detail by focusing on the stationary observations at the monitoring station to avoid confounding temporal and spatial variability. In 2023, the monitoring station observations span the entire spring to late-autumn period, making these time series suitable for further analysis. From monitoring station time series, we saw the aforementioned

https://doi.org/10.5194/egusphere-2025-1492
Preprint. Discussion started: 4 April 2025

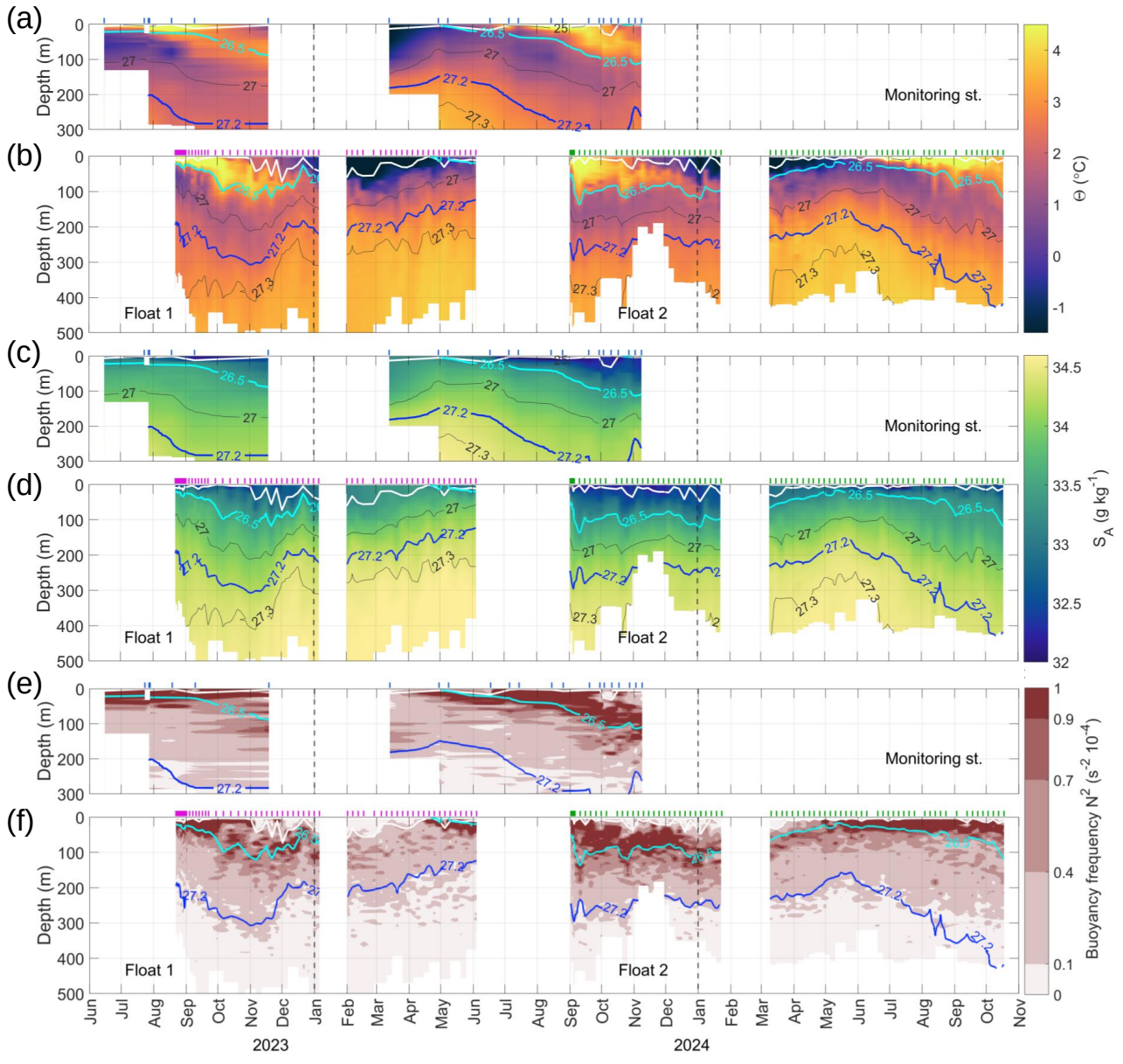

Figure 3. Hydrography in Disko Bay from June 2022 to October 2024. Temperature for the monitoring station (a) and profiling floats (b). Salinity for the monitoring station (c) and profiling floats (d). Buoyancy frequency for the monitoring station (e) and profiling floats (f). Temperature, Salinity, and Buoyancy Frequency are overlaid by labelled isopycnals (blue thick line σ_0= 27.2 kg m^{-3} showing the upper WGIW boundary) and mixed-layer depth (white lines). Vertical ticks on the upper x-axis in (a)-(f) show the time of profile acquisitions (blue - monitoring station, pink - Float 1, green - Float 2), while dashed vertical lines through all panels mark the start of each calendar year.

https://doi.org/10.5194/egusphere-2025-1492
Preprint. Discussion started: 4 April 2025

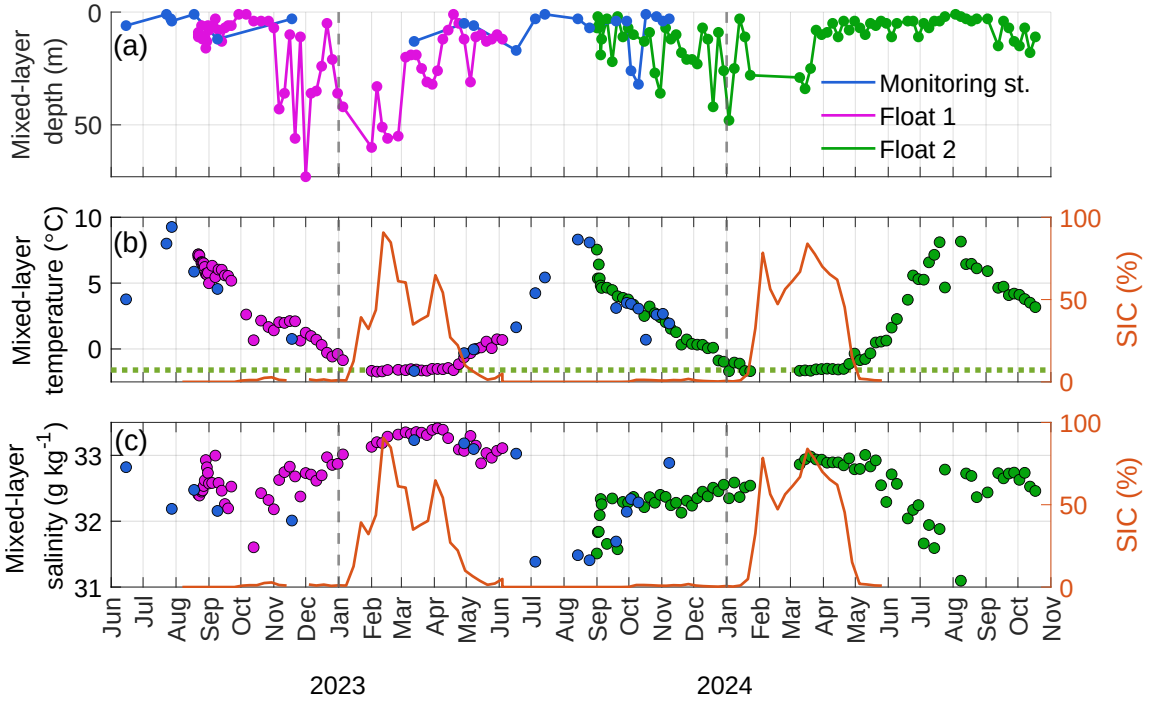

Figure 4. Time series of Disko Bay mixed-layer properties between 2022-2024, with a) Mixed-layer depth (MLD), b) mixed-layer temperature, and c) mixed-layer salinity. Sea-ice concentration inside Disko Bay is shown in orange in b) and c). Observed profiles are from the monitoring station (blue) and two floats (pink - Float 1, green - Float 2).

seasonal development, with a fresh stratified subsurface layer confined to the upper 50m during summer and its deepening at the start of September (Fig. 3c,f; green star markers in Fig. 5).

We further examine these changes at the monitoring station with Θ-S_A diagram (Fig. 6). Alongside freshening in the $\sigma_0 <$ 26.5 kg m^{-3} density range (grey shading in Fig. 6), temperatures in this density range increased through the summer, peaking in September before beginning to cool over autumn. In contrast, the PW in the $\sigma_0 =$ 26.5-27.1 kg m^{-3} (yellow shading in Fig. 6) continued to warm from September to November. Given that this warming is decoupled from the autumn cooling in the upper layers, we hypothesise that it could be advected.

4.3.2 Spatial variability in Polar Water across the bay

We investigate the hypothesis that the increasingly warm PW with densities between $\sigma_0 =$ 26.5-27.1 kg m^{-3} is advected towards the monitoring station through autumn (Fig. 6). We do that with a spatial analysis by incorporating additional data from two near-synoptic surveys conducted during the summer of 2018 (Fig. 7a). These surveys cover much of the deep basin of Disko Bay. We group the observations from May and August into three regions based on bathymetry and a priori knowledge of the general circulation. The regions are defined as eastern, northern, and central (coloured boxes in Fig. 7a). The eastern

https://doi.org/10.5194/egusphere-2025-1492
Preprint. Discussion started: 4 April 2025

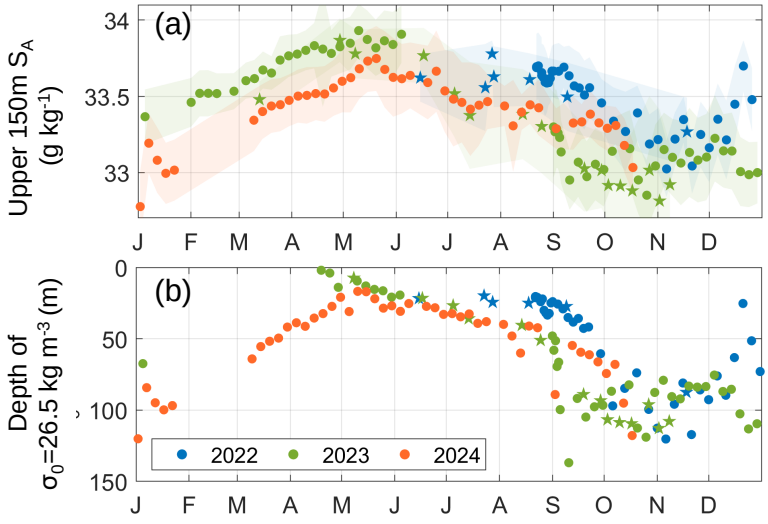

Figure 5. Seasonal cycle of (a) mean salinity in the upper 150m, with one standard deviation shaded in the background, and (b) depth of the $\sigma_0 = 26.5$ kg m^{-3} isopycnal, which approximates the extent of the stratified layer. The seasonal cycles of 2022, 2023, and 2024 are shown with blue, green, and orange markers, respectively. Star markers are for the monitoring station observations, and circles for the Float 1 and 2.

region is located near the Ilulissat Icefjord, while the northern region follows the outflow path dictated by the bay's bathymetry and circulation. The central region covers the deeper basin of Disko Bay and is thought to be the centre of the cyclonic circulation within the bay. We compare temperature and salinity within these regions and track their changes from May to August (Fig. 7b-d,f-h).

In May, the central and northern areas displayed similar hydrographic characteristics (Fig. 7 b-d). However, in the east, the PW temperature gradient was less pronounced (Fig. 7 b). At depths where other regions exhibited a well-defined PW temperature minimum, the PW in the eastern area was ∼0.5°C warmer. Additionally, the upper 25 m in the east were notably fresher and colder than in the other areas (Fig. 7 b,c).

By August, all three regions were distinctly different (Fig. 7 f-h). Below the freshened upper layer, the central area maintained a similar hydrographic structure as in May. Its density profile remained largely the same (Fig. 7 h) and a well-defined PW temperature minimum was at the same depths as before (Fig. 7 f). The northern and eastern areas showed more significant changes. In both of these areas, PW had warmed at intermediate depths (50-150m in the east, upper 100m in the north, Fig. 7 f), and there were also changes in salinity and density, with the eastern region showing more significant changes compared to the north (Fig. 7 g,h). The surface layer remained the coldest and freshest in the east(Fig. 7 f,g).

Although there is a temporal development, the overall spatial patterns remain consistent. In the eastern region, near Ilulissat Icefjord, the uppermost layer is notably colder, while the underlying PW is warmer and exhibits a less pronounced temperature minimum compared to other regions. A similar but weaker pattern is observed in the northern part of the bay. In contrast,

https://doi.org/10.5194/egusphere-2025-1492
Preprint. Discussion started: 4 April 2025

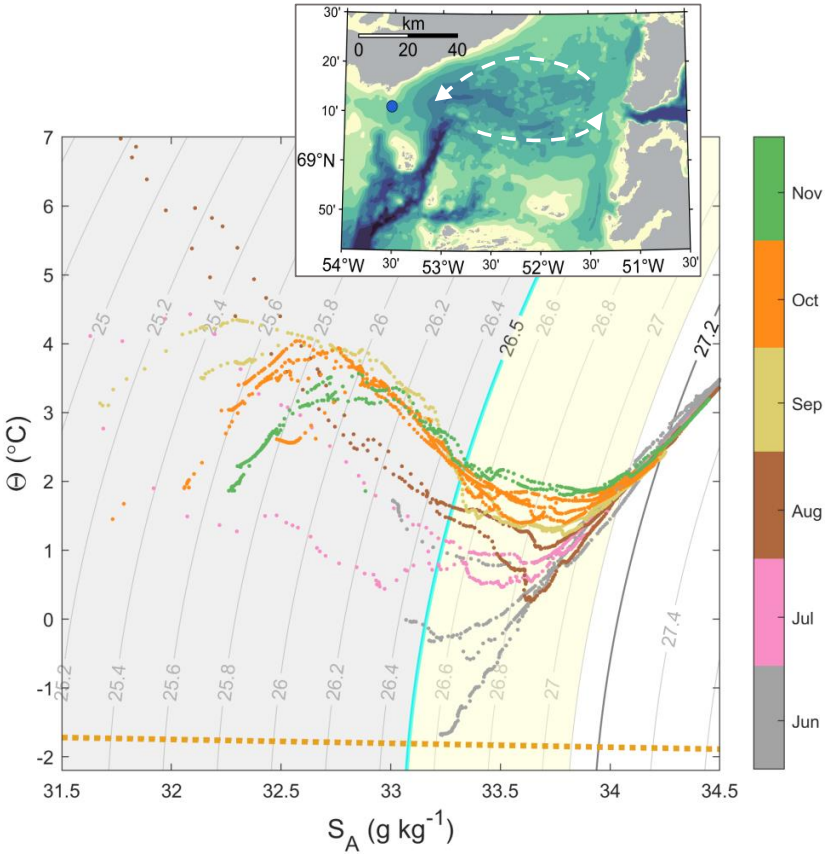

Figure 6. Theta-SA diagram showing observed temperature and salinity from the monitoring station (blue circle in inset map) spanning June to November 2023 (circle markers coloured by month). Grey contours show isopycnals, with 27.2 kg m^{-3} delineating West Greenland Irminger Water (WGIW) and Polar Water (PW). Grey shading above 26.5 kg m^{-3} marks the isopycnal range where PW is cooling through autumn, while yellow shading marks where along-isopycnal warming occurs simultaneously. The dotted orange line marks the surface freezing point.

the central region remains relatively stable, lacking the pronounced temperature anomalies seen in the eastern and northern regions.

However, comparing properties solely along the depth coordinate provides an incomplete view, as the isopycnals do not lie at the same depths across the bay (Fig. 7 d,h). Therefore, comparing properties along isopycnals rather than depth offers a more accurate representation. Thus, we calculate the along-isopycnal temperature anomaly in the eastern and northern regions by using the central part of the bay as a reference. We select the central area as a reference for two reasons: first, it is relatively unaffected by the anomalies seen in the east and north, and second, if these anomalies are advective, the centre of the bay lies outside the bay's cyclonic circulation pathway between the east and north.

https://doi.org/10.5194/egusphere-2025-1492
Preprint. Discussion started: 4 April 2025

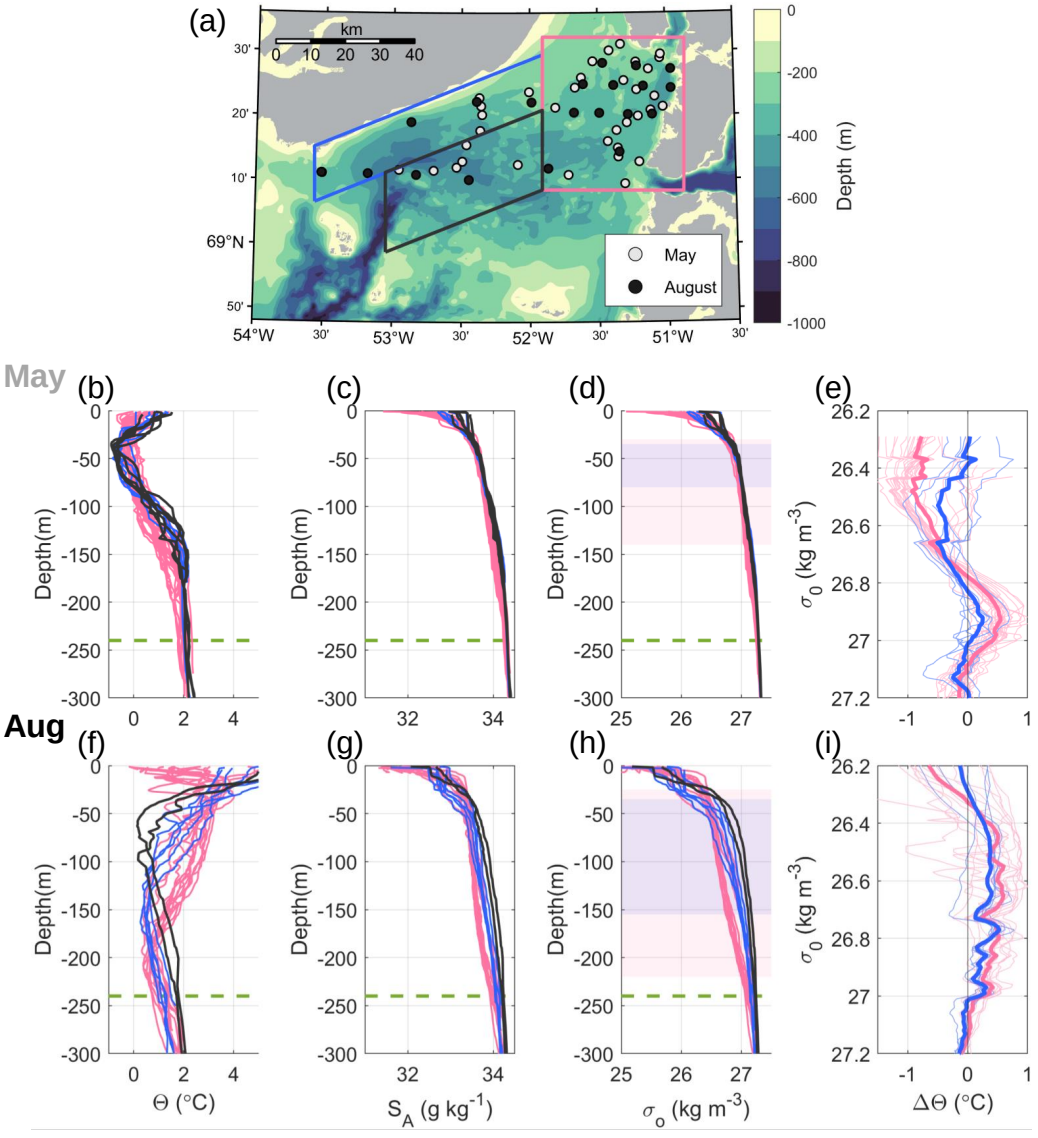

Figure 7. Spatial analysis of two survey cruises in Disko Bay in 2018. (a) The map shows survey stations from the May (grey dots) and August (black dots) cruises, divided into three regions: eastern (pink box), northern (blue box), and central (black box). The results are displayed for May (b–e) and August (f–i), depicting temperature (b, f), salinity (c, g), and density profiles (d, h), with each profile colour-coded by region. The green dashed line indicates the depth of the Ilulissat Icefjord Sill (240 m). Along-isopycnal temperature anomalies ($\Delta\Theta$) relative to the central region in May (e) and August (i) as a function of density, with thin lines showing $\Delta\Theta$ for each profile and a thick line showing the regional mean. Positive $\Delta\Theta$ anomalies are identified from the mean (e, i) and the depth range of these densities is shaded in (d,h), colour-coded by region.

https://doi.org/10.5194/egusphere-2025-1492
Preprint. Discussion started: 4 April 2025

The results reveal positive along-isopycnal temperature anomalies, especially in the eastern area (Fig. 7e,i). In May, the waters within the $\sigma_0 = 26.75\text{-}27.08$ kg m^{-3} density range were $\sim$0.5°C warmer in the east than in the centre (Fig. 7e). These densities occupy 30-140 m depth in this region (Fig. 7d). A similar anomaly was observed in the northern area within a narrower density range of $\sigma_0 = 26.85\text{-}27.01$ kg m^{-3} exhibiting anomalies of ~ 0.2°C (Fig. 7e, 30-80 m depth (Fig. 7d)). By August, the warm anomaly in the east extended across a broader density range of $\sigma_0 = 26.32\text{-}27.14$ kg m^{-3} with the anomaly of $\sim$0.55°C (Fig. 7i). These densities extend to 220 m (Fig. 7h). In the north, densities of $\sigma_0 = 26.29\text{-}27.01$ kg m^{-3} displayed similar anomalies of $\sim$0.4°C (Fig. 7i, 30-80 m depth (Fig. 7h)).

In summary, we identify warm along-isopycnal anomalies, indicating that in the east, near Ilulissat Icefjord, waters of the same density are warmer (and consequently more saline) than those in the centre of the bay. From May to August, this anomaly expanded occupying a broader density and depth range, and increasing in magnitude. A similar trend was observed further north along the outflow path, although over narrower density and depth range, and with a smaller magnitude. The findings suggest that along-isopycnal warming from the east may have propagated towards the northern region. Furthermore, the results show a temporal progression of these anomalies between May and August within the eastern region.

Assuming this spatial pattern is not a transient feature, we can use these results to interpret the along-isopycnal warming within the $\sigma_0 = 26.5\text{-}27.1$ kg m^{-3} density range observed at the monitoring station in autumn 2023 (Fig. 6). First, we can infer that this signal was likely advected from the east. Then, as spatial analysis showed this signal intensified between May and August 2018 in the east, the continued along-isopycnal warming at the monitoring station in the autumn of 2023 may be reflecting an advective delay.

Expanding this to the entire time series of 2022-2024, we note that along-isopycnal warming in autumn is a seasonal feature (Fig. 8). Over the three observed summer-autumn cycles, temperatures at two select deep isopycnals (σ_0 =26.8 kg m^{-3} and $\sigma_0 = 27$ kg m^{-3}) showed an increase in autumn. In 2024, the increase in along-isopycnal temperature commenced in August, possibly reflecting the closer proximity of the Float 2 that sampled that year to the eastern region.

4.4 Seasonality of West Greenland Irminger Water

At depths larger than 300 m, WGIW is isolated within Disko Bay, as it is confined by shallow bathymetric barriers around the bay (200m at the entrance to Vaigat Strait, 240 m at Ilulissat Icefjord and 300m at EDS (Fig.1b)). Regarded as basin water, WGIW can be renewed if equally dense or denser waters pass over the topographic constraints (Gade and Edwards, 1980), with the deepest and most applicable one being the EDS (Gladish et al., 2015a). As such, the onset of a WGIW renewal is seen as an increase in density below 300 m.

The first signs of WGIW renewal are seen in early November 2022, when the basin density at 400 m began to increase from the September-October mean of σ_0= 27.31 kg m^{-3} to σ_0= 27.36 kg m^{-3}, reached by early December 2022 (grey shading in Fig. 9e). Along with this increase in basin density, basin temperatures rose by $\sim 0.3°C$ (Fig. 9f). Around two weeks after the basin density began to increase, the upper boundary of WGIW rose rapidly, with $\sigma_0 = 27.2$ kg m^{-3} shoaling by >100 m within a span of two weeks (Fig. 9d), reflecting the uplift of lighter WGIW that previously resided in the basin. Prior to this renewal, a seasonal shift in prevailing wind direction occurred, whereby the along-coast (north-south) winds switched from

https://doi.org/10.5194/egusphere-2025-1492
Preprint. Discussion started: 4 April 2025

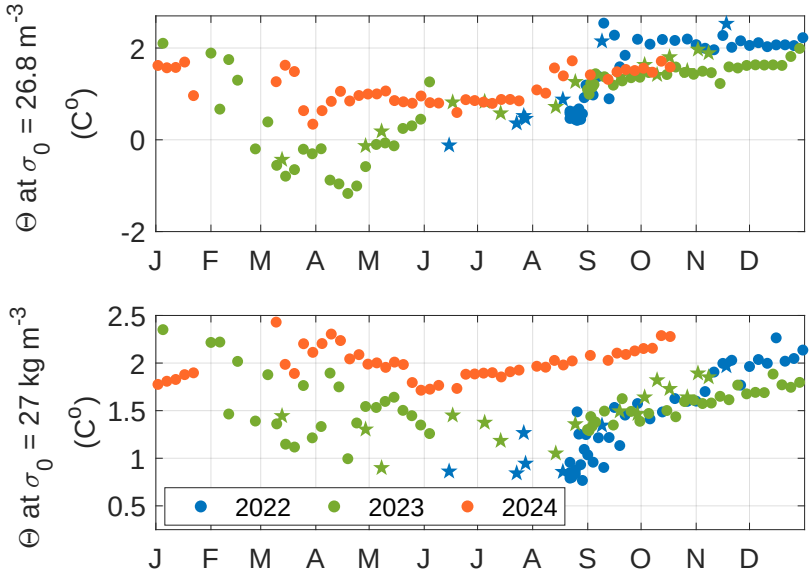

Figure 8. Seasonal cycle of along-isopycnal temperature at (a) $\sigma_0 = 26.8$ kg m^{-3} and (b) $\sigma_0 = 27$ kg m^{-3} isopycnals. The seasonal cycles of 2022, 2023, and 2024 are shown with blue, green, and orange markers, respectively. Star markers are for the monitoring station observations, and circles for the Float 1 and 2.

being predominantly southerly in summer to northerly in autumn to spring (from positive wind stress values to negative in Fig. 9b). In the absence of strong sea-ice cover, such northerly winds (negative wind stress) would lead to upwelling over the area of Egedesminde Dyb and its sill (EDS). Indeed, upwelling-favourable conditions persisted through November 2022 (positive vertical velocity in Fig. 9c), which appears to have lifted the dense waters to the west over EDS and led to the observed basin renewal in November-December 2022 (Fig. 9d-f).

In the following months of the winter 2022-2023, basin density did not increase as rapidly as in November and December. Still, a gradual increase from σ_0= 27.36 kg m^{-3} to σ_0= 27.39 kg m^{-3} was observed between February and late April 2023 (grey shading in Fig. 9e), indicating a sustained inflow over the EDS. Alongside this increase in density, basin temperatures rose by $\sim 0.5°C$, reaching the annual peak in WGIW temperature at the end of April 2023 (Fig. 9f). This ongoing dense renewal lifted the overlying WGIW, which then continued to rise until the start of June 2023 (Fig. 9d). This period corresponds to the annual maximum vertical extent of WGIW in Disko Bay, with $\sigma_0 = 27.2$ reaching ~100m depth in late May and early June 2023 (Fig. 9d). Northerly winds and positive vertical velocities persisted until the prevailing winds changed direction in mid-May 2023, ending the upwelling-favourable conditions (Fig. 9b,c).

During autumn and winter 2023-2024, basin waters did not increase in density and remained at σ_0= 27.3 kg m^{-3} (Fig. 9e). Northerly wind stress was weaker in September 2023-January 2024 compared to the previous year (Fig. 9b). Nevertheless, some positive vertical velocities were observed over the EDS area in October-November 2023 (Fig. 9c), coinciding with a slight 50m uplift of the WGIW boundary at the start of November (Fig. 9d). In March and April 2024, signs of renewal

https://doi.org/10.5194/egusphere-2025-1492
Preprint. Discussion started: 4 April 2025

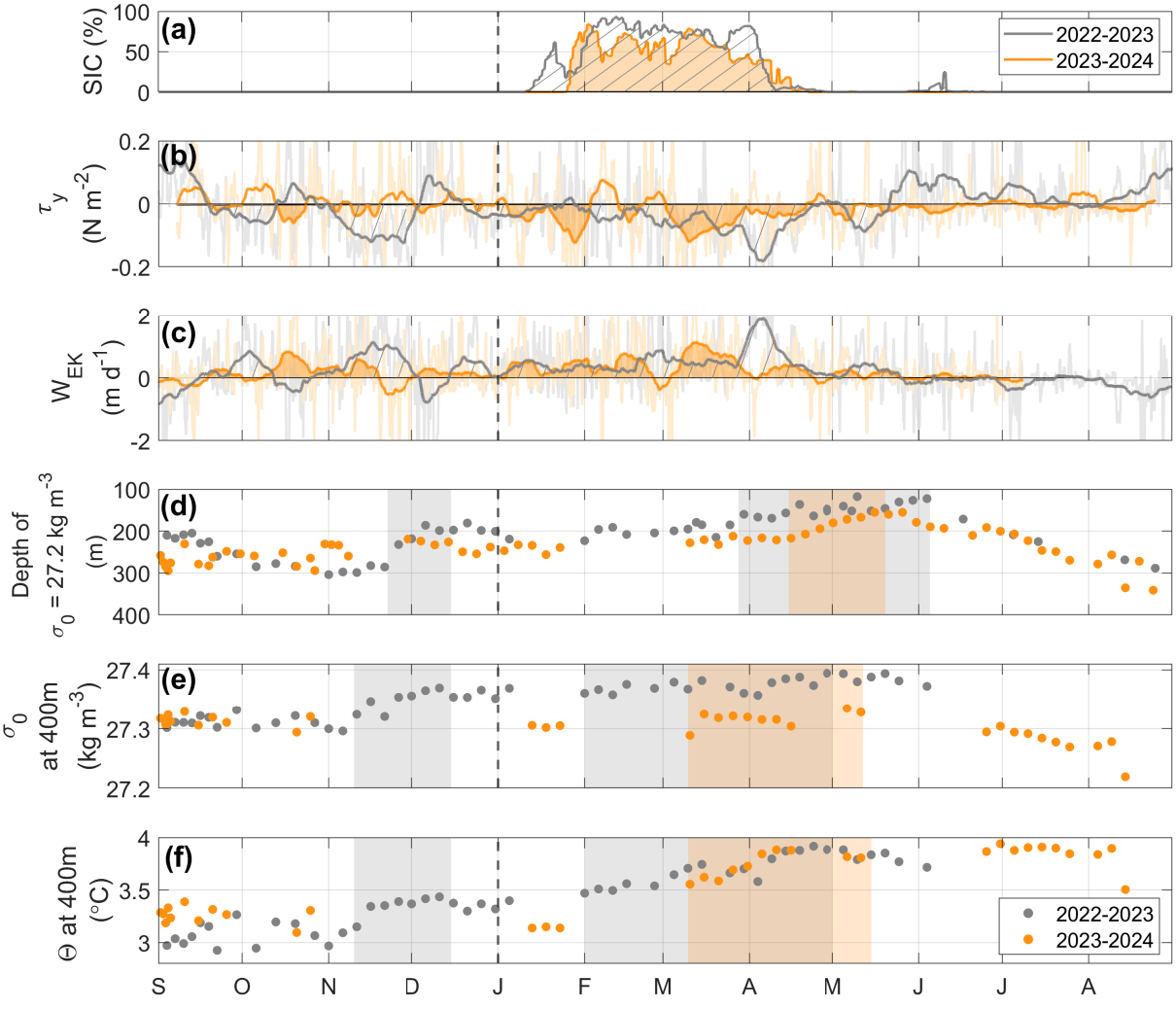

Figure 9. Seasonality of atmospheric forcing and WGIW properties in Disko Bay based on two annual cycles of observations (grey colours for 2022-2023, orange colours for 2023-2024). Mean sea-ice cover (a), along-shore wind stress (τ_y) (b), and vertical velocity W_E (Ekman pumping) over the EDS area (Fig. 1a) (c). In (b-c), hourly data in the background is overlaid by a 10-day running mean in thick lines. Shaded or hatched areas highlight the negative and positive ranges in (b) and (c), respectively. Depth of the σ_0= 27.2 kg m^{-3} - upper WGIW boundary (d) for all observations. Density (e) and temperature (f) at 400m depth. Background shading in (d-e) mark periods with renewal signatures, with grey for 2022-2023 renewals and orange for 2023-2024 renewals. The dashed vertical line in all plots marks a new year.

were observed, as basin density increased by 0.1 kg m^{-3} and temperature rose by approximately $\sim 0.5°C$ over one month (orange shading in Fig. 9e,f). However, wind forcing and upwelling were not evident during this period, suggesting a non-local mechanism behind this renewal. By the end of May and the start of June 2024, similar to spring 2023, this inflow resulted in the maximum observed vertical extent of WGIW (Fig. 9d).

https://doi.org/10.5194/egusphere-2025-1492
Preprint. Discussion started: 4 April 2025

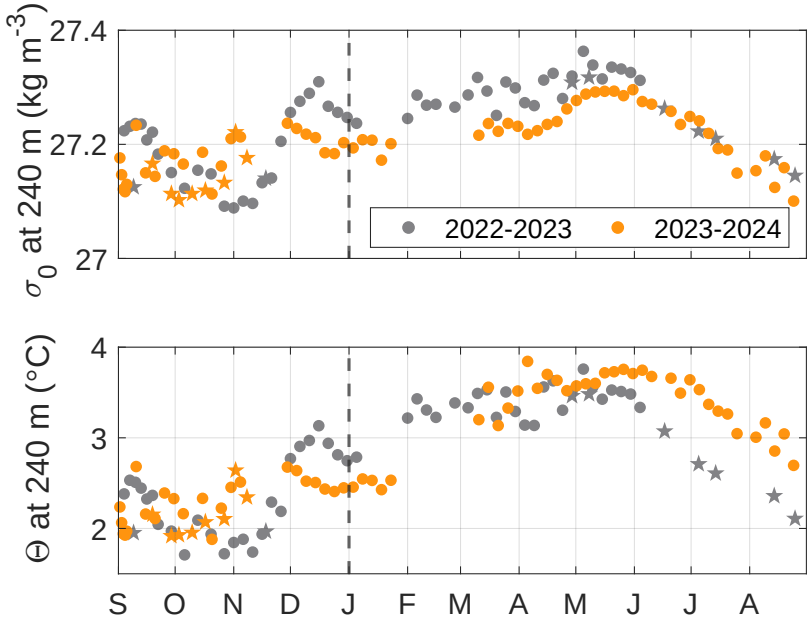

Figure 10. Seasonal cycle of density (a) and temperature (b) at 240m depth, corresponding to the Ilulissat Icefjord Sill depth. Grey markers are observations from 2022-2023 and orange from 2023-2024. Star markers are for the monitoring station observations, and circles for the Float 1 and 2.

In both years, the WGIW reached its maximum vertical extent in May-June, reaching 150 m in 2023 and 180 m in 2024 (Fig. 9d). This shoaling of the WGIW makes the warm waters available above the Ilulissat Icefjord sill depth (240 m). Observations at the same depth in Disko Bay show a seasonal temperature cycle of $\sim 2°C$, with a peak of $> 3.5°C$ in May-June (Fig. 10b). The density at 240 m depth follows a similar seasonal pattern, with a peak of σ_0= 27.3-27.35 kg m^{-3} in May/June and a minimum density of σ_0= 27.1 kg m^{-3} from August to November (Fig. 10a). We note that there is a spatial variability around these depths in August-November, previously highlighted in Sect. 4.3.2, which is also seen in a more extensive spread of observed densities and temperatures in the autumn of 2023-2024 cycle (Fig. 10a,b). These observations come from the monitoring station and Float 2 (star and circle markers, respectively, in Fig. 10a,b), thus reflecting the spatial variability. Overall, depending on the basin density in the Ilulissat Icefjord, the densest waters for Ilulissat Icefjord renewal are available in May/June. Additionally, a pronounced autumn WGIW renewal in Disko Bay, similar to the one observed in November-December 2022, can elevate the WGIW enough to drive a temperature increase of $\sim 1.5°C$ at the Ilulissat Icefjord sill depth Fig. 10b). This suggests that, at times, warm and dense waters could become available for renewal in the Ilulissat Icefjord as early as late autumn and early winter.

https://doi.org/10.5194/egusphere-2025-1492
Preprint. Discussion started: 4 April 2025

5 Discussion

Our results documented two full annual cycles of hydrographic properties within Disko Bay. In addition to the expected seasonality within the mixed layer, we observed notable seasonal variability within PW and seasonal inflow of dense WGIW. In what follows we discuss the sources of the observed signals and compare them to earlier relevant studies.

5.1 Phases of Polar Water seasonality

The seasonal cycle of PW and the mixed layer within follow three main phases. First, in winter and spring, cooling, sea-ice formation, and brine rejection increase the salinity in the mixed layer as it deepens (Fig. 4). Second, with the onset of summer and the melt season, a shallow and stratified layer develops, isolating PW below, which forms a characteristic temperature minimum in the water column. Finally, at the end of summer and into autumn, PW undergoes counter-intuitive changes. A fresh, stratified layer extends over the upper 150 m, causing isohalines to deepen as autumn progresses (Fig. 5). Additionally, throughout autumn, along-isopycnal warming is observed below this stratified, fresh layer (Fig. 6, Fig. 8). Thus, a two-way development in PW occurs in autumn: 1) a fresh, stratified layer that extends deeper and gradually cools and 2) below this, along-isopycnal warming.

While processes occurring in winter, spring, and summer are well understood, those in autumn warrant further discussion.

5.1.1 Deepening of fresh and stratified layer

One potential source of this deep fresh signal at the start of autumn is lateral advection of upstream waters with the WGC/WGCC. Observations from the Davis Strait mooring array show a clear annual cycle in salinity, with peak salinities along the west Greenland shelf between April-June (33.66 g kg^{-1}) and a decrease towards the annual minimum in August-October (32.75 g kg^{-1}) (Curry et al., 2014; Carroll et al., 2018). Deeper in the water column, at the shelf-slope at Davis Strait ($\sim$ 150 m) the salinity follows the same annual cycle (Gladish et al., 2015a). Given that Davis Strait is 400 km south of Disko Bay and the subsurface velocity of WGC is around 0.07 m s^{-1} in autumn (Curry et al., 2014), these signals are expected to reach Disko Bay with a delay of about two months. This timing aligns well with the observed seasonality in Disko Bay, where we see a fresh signal extending over the upper 150 m at the start of autumn (Fig. 5), i.e. two months after the onset of decreasing salinities along the shelf. Therefore, the seasonal feature observed in Disko Bay may reflect the influence of freshwater advected by the WGC/WGCC. However, typical minimum density and salinity at $\sim$ 150 m in Davis Strait tends to be higher ($\sigma_0 > 27$ kg m^{-3} and $S_A > 33.8$)(Gladish et al., 2015a), compared to what we observe at the same depth in Disko Bay during autumn (Fig. 3c,d). Therefore, an additional source of fresh signals may be more localised within Disko Bay.

The Ilulissat Icefjord significantly contributes to freshwater fluxes, which originate from three primary sources in the fjord. The first source is glacial runoff that enters the fjord at depth as SGD. The other two are the underwater melting of the glacier terminus and melting icebergs, both of which form the SMW component. These freshwater fluxes vary in magnitude seasonally. The most substantial contributor is the melting of icebergs within the fjord, with estimates increasing from 700-1000 m^3s^{-1} during winter to a peak of 1200-1800 m^3s^{-1} in August (Enderlin et al., 2016; Kajanto et al., 2023). The second-largest

https://doi.org/10.5194/egusphere-2025-1492
Preprint. Discussion started: 4 April 2025

contribution comes from SGD, which has near-zero fluxes in winter that rise to around 900 m^3s^{-1} in summer (Mernild et al., 2015; Enderlin et al., 2016). The SMW contribution from terminus melt remains highly uncertain, as it is influenced by seasonal variations in SGD. In the summer, a buoyant plume generated by SGD enhances melting at the terminus, boosting its SMW contribution to a peak of about 70-400 m^3s^{-1} (Enderlin et al., 2016; Kajanto et al., 2023). In winter, with near-zero SGD, terminus melt is similar to that of icebergs. However, since the area of the submerged glacier terminus is at least an order of magnitude smaller than the submerged area of icebergs (9-27 km^2 for the submerged terminus versus 470-690 km^2 for icebergs), the contribution of SMW from terminus melt is relatively minor in winter (Enderlin et al., 2016).

A mix of these melt products, PW, and WGIW, forms a new water mass GMW. The GMW that exits from Ilulissat Icefjord into Disko Bay flows north as a buoyant stratified current (Beaird et al., 2017). This current features a cold, fresh, stratified layer that extends to at least 100 m deep near the shore, as observed in August 2014 by Beaird et al. (2017). They noted that the concentration of meltwater decreased offshore, resulting in a shoaling of the GMW layer; however, the upper 35 m retained the cold and fresh GMW signature up to 10 km offshore. We refrain from directly comparing our results from the 2018 cruises with the data from 2014, as the conditions in 2018 were notably different. 2018 was an anomalously cold year in Disko Bay (Khazendar et al., 2019; Joughin et al., 2020); this can be seen when comparing temperature profiles in 2022-2024 (Fig. 2b) and 2018 (Fig. 7b,f). However, our results do indicate a similar cold and fresh anomaly in May and August 2018 near the Ilulissat Icefjord. We also observed this anomaly propagating further north and west as it moved downstream. Thus, the export of thick meltwater-laden GMW in the upper layers could be an additional reason for the seasonally observed freshening and deeper extension of the stratified layer at the start of autumn, considering that the peak melt season in the fjord occurs around August.

Finally, this fresh anomaly may partly be maintained by the continued melting of the icebergs within Disko Bay, where a high density of icebergs persists year-round (Enderlin et al., 2016; Scheick et al., 2019). The annual average solid ice discharge at the terminus of Sermeq Kujalleq is around 50 Gt/yr, which equates to $\sim$ 1500 m^3s^{-1} (Mankoff et al., 2020). Given the annual average iceberg melt inside the fjord is $\sim$ 1200 m^3s^{-1} (Kajanto et al., 2023), it suggests that up to 80% of icebergs may already melt inside Ilulissat Icefjord. The remaining icebergs, however, can cross over the sill and enter Disko Bay. Inside Disko Bay, the iceberg size distribution is predominantly made up of smaller icebergs. At times, more than 1000 small icebergs (with an area of about 1800 m^2), can be observed simultaneously (Scheick et al., 2019). Assuming an average rectangular iceberg of this size, its length would be $\sim$ 130 m, height $\sim$ 65 m (based on aspect ratios of typical icebergs in Ilulissat Icefjord (Enderlin et al., 2016)), and draft $\sim$ 55 m (Cenedese and Straneo, 2023). Given the average summertime temperature of 2°C in the upper 50 m, and assuming fully turbulent conditions around the iceberg, we estimate that the upper bound of summertime meltwater flux from 1000 of these icebergs would be around 65 m^3s^{-1}. This indicates that while iceberg melting during summer in the bay is significant, it is not the primary source of freshwater.

5.1.2 Along-isopycnal warming at depth

The glacial influence may also explain the deep warm along-isopycnal anomalies we observed, which were most pronounced near Ilulissat Icefjord in 2018 surveys (Fig. 7 e,i). Typically, the characteristic warm signature of GMW arises from the en-

https://doi.org/10.5194/egusphere-2025-1492
Preprint. Discussion started: 4 April 2025

trainment of WGIW, which contributes a significant fraction of the water masses present in the GMW layer, while meltwater (SGD and SMW) remains highly diluted and is not dominant. For example, GMW exported from Ilulissat Icefjord contains about 40% WGIW (Beaird et al., 2017). As a result, GMW is generally warmer and more saline than unmodified water of the same density (Beaird et al., 2018; Muilwijk et al., 2022; Cowton et al., 2023).

Although we cannot directly quantify the specific contributions of water masses to GMW, the observed anomalies suggest the presence of WGIW at depths typically occupied by PW. A warm along-isopycnal anomaly was observed at depths of 30-134 m in May near Ilulisat Icefjord (Fig. 7 d,e), which deepened to 50-220 m by August (Fig. 7 h,i). Since this anomaly occurred at depths shallower than the Ilulissat Icefjord sill, it is possibly sourced from the fjord itself. Similar warm anomalies have been identified in numerous glacial fjords along northwest Greenland (Muilwijk et al., 2022; Cowton et al., 2023) and in southeast Greenland (Beaird et al., 2018). The deepening of this layer from May to August aligns with model results by Cowton et al. (2023), which suggest that as subglacial discharge decreases in late summer and autumn, the GMW plume's neutral buoyancy shifts to greater depths.

If an anomaly exists outside the Ilulissat Icefjord, it would circulate Disko Bay following the general cyclonic flow. This is then consistent with a warm anomaly of GMW origin exported from the Ilulissat Icefjord, carried with the cyclonic circulation around the bay at its isopycnic level, and later arriving further downstream (e.g. monitoring station in autumn 2023 (Fig. 6)). Furthermore, we observed that along-isopycnal warming was a seasonal feature in all three sampled autumns, indicating that it was not a transient feature (Fig. 8).

5.2 West Greenland Irminger Water renewal

Our observations over two annual cycles (2022-2023, 2023-2024) show that seasonal WGIW renewal occurs in spring. We demonstrate that during spring, the densest WGIW fills the Disko Bay basin, resulting in maximum temperature and salinity, as well as the greatest vertical extent of WGIW observed throughout the year (Fig. 9d-f). The springtime renewal process begins in February/March and reaches its peak by May/June in both years. This provides direct observational evidence supporting the hypothesis proposed by Gladish et al. (2015a, b), who suggested that exchange over the EDS likely occurs in spring. Indeed, we observed the arrival of the densest WGIW in spring, which has also been observed further north along the West Greenland coast (Carroll et al., 2018).

The repeated springtime renewal of dense WGIW in Disko Bay aligns with the broader annual WGIW cycle and the vertical isopycnal displacement of about 140m at the shelfbreak in Davis Strait (Curry et al., 2011, 2014; Gladish et al., 2015b; Carroll et al., 2018). During spring, isopycnals over the West Greenland slope and shelf exhibit an upward tilt toward the Greenland shelf, coinciding with densification of WGIW along the shelf that reaches its maximum in April at Davis Strait (Curry et al., 2014; Gladish et al., 2015a). As a result, increasingly dense waters may become available over the EDS, eventually exceeding the density of resident basin waters in Disko Bay and renewing the basin during spring.

Our results also suggest that WGIW renewal can occur following periods of upwelling-favourable winds. We observed clear signs of renewal in late autumn of 2022, marked by a rapid increase in basin density and temperature, followed by a notable vertical increase in the thickness of the WGIW layer within the bay (Fig. 9d-f). This autumn/winter renewal was unique to the

https://doi.org/10.5194/egusphere-2025-1492
Preprint. Discussion started: 4 April 2025

2022-2023 annual cycle and coincided with upwelling-favourable winds over the EDS area. These conditions likely induced upwelling near the EDS, lifting the dense waters over the topographic constraint and facilitating their access into Disko Bay. We estimated the upwelling velocity during the favorable period to about 1 m day^{-1} or a total uplift during the period of around 15 m, but the upwelling velocities may be larger than the values obtained using Eq. 5 since EDS is located relatively close to the coast, so that coastal upwelling may play a role. Similarly, Carroll et al. (2018) attributed the increased presence of WGIW in the Uummannaq trough, located 300 km north of Disko Bay, to upwelling-favourable conditions in Baffin Bay during December-January. Our results indicate that this mechanism of WGIW transport into Disko Bay may increase the density at depths above the Ilulissat Icefjord sill earlier in the year than previously expected (Gladish et al., 2015a, b).

5.3 The significance of the unravelled seasonality

The enhanced understanding of hydrographic seasonality presented here aids in interpreting long-term time series from Disko Bay, particularly those from continuous monitoring at its northwestern end (GEM monitoring station). A better understanding of the seasonality locally enables the de-seasoning of these time series. Our results also help evaluate the observations in a spatial context. Specifically, we find that waters exported from Ilulissat Icefjord are transported further into the bay by the general circulation, likely reaching as far as the monitoring station. While the lack of velocity observations prevents precise quantification of the advective timescale, we estimate that signals from Ilulissat Icefjord take a few weeks to arrive there.

Since the 2000s, increased meltwater delivery has contributed to higher primary production in Disko Bay, and the upwelling related to glacial processes has been shown to influence coastal phytoplankton dynamics in the bay as far as up to 50 km offshore (Oliver et al., 2023). Nutrients are upwelled and entrained into GMW within Ilulissat Icefjord (Hopwood et al., 2025), and we have described how this watermass spreads out into the bay spatially and seasonally. The nutrients are transported into the Disko Bay and subsequently into Ilulissat Icefjord with the nutrient-rich WGIW, making our findings on WGIW renewal directly relevant to marine biology.

Finally, an improved understanding of seasonality can provide an important context for interpreting the seasonal phenology of marine organisms within the bay, as well as for modelling and observational efforts to resolve Ilulissat Icefjord dynamics, now and in the future.

6 Conclusions

This paper examines hydrographic seasonality in Disko Bay using observations from summer 2018 and the June 2022–October 2024 period. Our findings reveal a consistent seasonal cycle, spanning from the surface mixed layer to deep waters, that governs annual hydrographic variability in the bay. By integrating data from a monitoring station, regional surveys, and profiling floats, we provide a comprehensive picture of seasonal and regional influences on the bay's hydrography. The interplay between glacial outflow from the east and water-mass exchange from the west varies across space, depth, and time, shaping the bay's hydrography throughout the year.

https://doi.org/10.5194/egusphere-2025-1492
Preprint. Discussion started: 4 April 2025

Surface layer warming and freshening begin with sea ice melt. A shallow stratified surface layer reaches a maximum of ∼8°C and a salinity minimum of ∼31 g kg^{-1}. Spatially, surface mixed layer varies across the bay, with the coldest and freshest waters found in the vicinity of Ilulissat Icefjord.

The significant seasonal and regional differences within the bay are within Polar Water (PW), also below the mixed layer. PW exhibits a distinct annual salinity cycle of ∼0.8 g kg^{-1}, with decreasing salinity from summer to late autumn. We suggest this signal reflects substantial seasonal freshwater fluxes in the Ilulissat Icefjord and Disko Bay system.

In addition to salinity variations, autumn along-isopycnal warming of the PW core is consistent with the influence of Glacially Modified Water (GMW), which reflects the presence of entrained warm WGIW into the buoyant glacial plume. Such glacial influence is most substantial in the east of Disko Bay, where exchange between Disko Bay and Ilulissat Icefjord occurs. We found that this warm along-isopycnal anomaly circulates cyclonicly within the bay and propagates along the outflow path.

Our observations reveal that West Greenland Irminger Water (WGIW) renewal occurs annually in spring, with one episodic renewal also observed in late autumn. In spring, the densest WGIW fills the Disko Bay basin, peaking in temperature, salinity, and vertical extent by late spring/early summer. This provides observational evidence that WGIW renews in Disko Bay in spring, reflecting the seasonality of WGIW within West Greenland Current. An early renewal event observed in late autumn 2022, likely driven by upwelling-favourable winds, suggests an additional mechanism and timing of occasional WGIW renewal in Disko Bay.

This new, observation-based understanding of seasonality provides a foundation for more accurate predictions of future variability. The significant impacts of both local and remote influences on the bay must be considered to make reliable predictions for the air-ice-ocean connectivity and its implications for the marine ecosystem of this region.

Data availability. The merged MODIS-AMSR2 sea-ice concentration data is available at: https://data.seaice.uni-bremen.de/modis_ amsr2. Greenland Ecosystem Monitoring (GEM) data is available at: https://data.g-e-m.dk/datasets. Additional observations collected for this study at the monitoring station in 2023 will be available through the GEM database. ERA5 data are available at the Copernicus Climate Change Service (C3S) Climate Data Store (CDS) (https://doi.org/10.24381/cds.adbb2d47, Copernicus Climate Change Service, Climate Data Store, 2023). Bathymetry data is available from the NASA National Snow and Ice Data Center Distributed Active Archive Center at: https://doi.org/10.5067/849. Oceans Melting Greenland Data for the profiling floats is available at: https://podaac.jpl.nasa.gov/dataset/OMG_L1_FLOAT_ALAMO.
Greenland Ocean Observations Apex-float data is available at: https://fleetmonitoring.euro-argo.eu/float/6990591.

Author contributions. LL: Writing – review and editing, Writing – original draft, Visualization, Methodology, Investigation, Formal analysis, Conceptualization. LH: Writing - review and editing, Writing – original draft, Methodology, Investigation, Conceptualization, Supervision. ED: Writing - review and editing, Writing – original draft, Visualization, Methodology, Investigation. PJH: Writing - review and editing, Resources, Data curation. JKW: Writing - review and editing, Resources, Data curation

https://doi.org/10.5194/egusphere-2025-1492
Preprint. Discussion started: 4 April 2025

Competing interests. The authors declare that they have no conflict of interest.

Acknowledgements. We thank Dana Margareta King for processing the sea-ice data, Iliana Vasiliki Ntinou for assisting with the fieldwork, and Torkel Gissel Nielsen for support with planning the fieldwork. We gratefully acknowledge the crew of RV $Porsild$ and the staff at the Arctic Station (University of Copenhagen) in Qeqertarsuaq for their hard work and expertise in safely and effectively carrying out the fieldwork. We thank NASA OMG Mission, as well as the GEM programme for making observational data freely available. We acknowledge the collaborative efforts of scientists at the Greenland Institute of Natural Resources in collecting the NASA and NOAA "Greenland Ocean Observations" (GOO) float data that contributed to this study. This work was carried out in part at the Jet Propulsion Laboratory, California Institute of Technology, under a contract with the National Aeronautics and Space Administration (80NM0018D0004). This work was supported financially by the Research Council of Norway through the project ClimateNarratives (no. 324520).

https://doi.org/10.5194/egusphere-2025-1492
Preprint. Discussion started: 4 April 2025

References

Andersen, O. G. N.: The annual cycle of temperature, salinity, currents and water masses in Disko Bugt and adjacent waters, West Greenland, Meddelelser om Grønland. Bioscience, 5, 1–33, https://doi.org/10.7146/mogbiosci.v5.142180, 1981a.

Andersen, O. G. N.: The annual cycle of phytoplankton primary production and hydrography in the Disko Bugt area, West Greenland, Meddelelser om Grønland. Bioscience, 6, 1–65., https://doi.org/10.7146/mogbiosci.v6.142187, 1981b.

Argo: Argo float data and metadata from Global Data Assembly Centre (Argo GDAC), https://doi.org/10.17882/42182, 2024.

Beaird, N., Straneo, F., and Jenkins, W.: Characteristics of meltwater export from Jakobshavn Isbræ and Ilulissat Icefjord, Annals of Glaciology, 58, 107–117, https://doi.org/10.1017/aog.2017.19, 2017.

Beaird, N., Straneo, F., and Jenkins, W.: Export of Strongly Diluted Greenland Meltwater From a Major Glacial Fjord, Geophysical Research Letters, 45, 4163–4170, https://doi.org/10.1029/2018GL077000, 2018.

Carroll, D., Sutherland, D. A., Curry, B., Nash, J. D., Shroyer, E. L., Catania, G. A., Stearns, L. A., Grist, J. P., Lee, C. M., and de Steur, L.: Subannual and Seasonal Variability of Atlantic-Origin Waters in Two Adjacent West Greenland Fjords, Journal of Geophysical Research: Oceans, 123, 6670–6687, https://doi.org/10.1029/2018JC014278, 2018.

Cenedese, C. and Straneo, F.: Icebergs Melting, Annual Review of Fluid Mechanics, 55, 377–402, https://doi.org/10.1146/annurev-fluid-032522-100734, 2023.

Cowton, T. R., Slater, D. A., and Inall, M. E.: Subglacial-Discharge Plumes Drive Widespread Subsurface Warming in Northwest Greenland's Fjords, Geophysical Research Letters, 50, e2023GL103 801, https://doi.org/10.1029/2023GL103801, 2023.

Curry, B., Lee, C. M., and Petrie, B.: Volume, Freshwater, and Heat Fluxes through Davis Strait, 2004–05, https://doi.org/10.1175/2010JPO4536.1, 2011.

Curry, B., Lee, C. M., Petrie, B., Moritz, R. E., and Kwok, R.: Multiyear Volume, Liquid Freshwater, and Sea Ice Transports through Davis Strait, 2004–10, https://doi.org/10.1175/JPO-D-13-0177.1, 2014.

Enderlin, E. M., Hamilton, G. S., Straneo, F., and Sutherland, D. A.: Iceberg meltwater fluxes dominate the freshwater budget in Greenland's iceberg-congested glacial fjords, Geophysical Research Letters, 43, 11,287–11,294, https://doi.org/10.1002/2016GL070718, 2016.

Foukal, N. P. and Pickart, R. S.: Moored Observations of the West Greenland Coastal Current along the Southwest Greenland Shelf, https://doi.org/10.1175/JPO-D-23-0104.1, 2023.

Gade, H. G.: Melting of Ice in Sea Water: A Primitive Model with Application to the Antarctic Ice Shelf and Icebergs, https://journals.ametsoc.org/view/journals/phoc/9/1/1520-0485_1979_009_0189_moiisw_2_0_co_2.xml, 1979.

Gade, H. G. and Edwards, A.: Deep Water Renewal in Fjords, in: Fjord Oceanography, edited by Freeland, H. J., Farmer, D. M., and Levings, C. D., pp. 453–489, Springer US, Boston, MA, https://doi.org/10.1007/978-1-4613-3105-6_43, 1980.

Gladish, C. V., Holland, D. M., and Lee, C. M.: Oceanic Boundary Conditions for Jakobshavn Glacier. Part II: Provenance and Sources of Variability of Disko Bay and Ilulissat Icefjord Waters, 1990–2011, Journal of Physical Oceanography, 45, https://doi.org/10.1175/JPO-D-14-0045.1, 2015a.

Gladish, C. V., Holland, D. M., Rosing-Asvid, A., Behrens, J. W., and Boje, J.: Oceanic Boundary Conditions for Jakobshavn Glacier. Part I: Variability and Renewal of Ilulissat Icefjord Waters, 2001–14, Journal of Physical Oceanography, 45, https://doi.org/10.1175/JPO-D-14-0044.1, 2015b.

Gou, R., Pennelly, C., and Myers, P. G.: The Changing Behavior of the West Greenland Current System in a Very High-Resolution Model, Journal of Geophysical Research: Oceans, 127, e2022JC018 404, https://doi.org/10.1029/2022JC018404, 2022.

https://doi.org/10.5194/egusphere-2025-1492
Preprint. Discussion started: 4 April 2025

Greenland Ecosystem Monitoring: MarineBasis Disko - Water column - CTD measurements (Version 1.0) [Data set], https://doi.org/10.17897/WH30-HT61, 2025a.

Greenland Ecosystem Monitoring: MarineBasis Disko - Water column - Disko Bay Cruise 2018, CTD measurements (Version 1.0). [Data set], https://doi.org/10.17897/75KS-G922, 2025b.

Hansen, M. O., Nielsen, T. G., Stedmon, C. A., and Munk, P.: Oceanographic regime shift during 1997 in Disko Bay, Western Greenland, Limnology and Oceanography, 57, 634–644, https://doi.org/10.4319/lo.2012.57.2.0634, 2012.

Hersbach, H., Bell, B., Berrisford, P., Biavati, G., Horányi, A., Muñoz Sabater, J., Nicolas, J., Peubey, C., Radu, R., Rozum, I., Schepers, D., Simmons, A., Soci, C., Dee, D., and Thépaut, J-N.: ERA5 hourly data on single levels from 1940 to present, DOI:10.24381/cds.adbb2d47, 2023.

Holland, D. M., Thomas, R. H., de Young, B., Ribergaard, M. H., and Lyberth, B.: Acceleration of Jakobshavn Isbræ triggered by warm subsurface ocean waters, Nature Geoscience, 1, 659–664, https://doi.org/10.1038/ngeo316, 2008.

Hopwood, M. J., Carroll, D., Gu, Y., Huang, X., Krause, J., Cozzi, S., Cantoni, C., Gastelu Barcena, M. F., Carroll, S., and Körtzinger, A.: A Close Look at Dissolved Silica Dynamics in Disko Bay, West Greenland, Global Biogeochemical Cycles, 39, https://doi.org/10.1029/2023GB008080, 2025.

Huang, J., Pickart, R. S., Bahr, F., McRaven, L. T., Tremblay, J.-, Michel, C., Jeansson, E., Kopec, B., Welker, J. M., and Ólafsdóttir, S. R.: Water mass evolution and general circulation of Baffin Bay: Observations from two shipboard surveys in 2021, Progress in Oceanography, p. 103322, https://doi.org/10.1016/j.pocean.2024.103322, 2024.

Joughin, I., Shean, D. E., Smith, B. E., and Floricioiu, D.: A decade of variability on Jakobshavn Isbræ: ocean temperatures pace speed through influence on mélange rigidity, The Cryosphere, 14, 211–227, https://doi.org/10.5194/tc-14-211-2020, 2020.

Kajanto, K., Straneo, F., and Nisancioglu, K.: Impact of icebergs on the seasonal submarine melt of Sermeq Kujalleq, The Cryosphere, 17, 371–390, https://doi.org/10.5194/tc-17-371-2023, 2023.

Khazendar, A., Fenty, I. G., Carroll, D., Gardner, A., Lee, C. M., Fukumori, I., Wang, O., Zhang, H., Seroussi, H., Moller, D., Noël, B. P. Y., van den Broeke, M. R., Dinardo, S., and Willis, J.: Interruption of two decades of Jakobshavn Isbrae acceleration and thinning as regional ocean cools, Nature Geoscience, 12, 277–283, https://doi.org/10.1038/s41561-019-0329-3, 2019.

Ludwig, V., Spreen, G., and Pedersen, L. T.: Evaluation of a New Merged Sea-Ice Concentration Dataset at 1 km Resolution from Thermal Infrared and Passive Microwave Satellite Data in the Arctic, Remote Sensing, 12, 3183, https://doi.org/10.3390/rs12193183, 2020.

Lüpkes, C. and Birnbaum, G.: 'Surface Drag in the Arctic Marginal Sea-ice Zone: A Comparison of Different Parameterisation Concepts', Boundary-Layer Meteorology, 117, 179–211, https://doi.org/10.1007/s10546-005-1445-8, 2005.

Mankoff, K. D., Solgaard, A., Colgan, W., Ahlstrøm, A. P., Khan, S. A., and Fausto, R. S.: Greenland Ice Sheet solid ice discharge from 1986 through March 2020, Earth System Science Data, 12, 1367–1383, https://doi.org/10.5194/essd-12-1367-2020, 2020.

McDougall, T. J. and Barker, P. M.: Getting started with TEOS-10 and the Gibbs Seawater (GSW) Oceanographic Toolbox, 28pp, www.TEOS-10.org, 2011.

Mernild, S. H., Holland, D. M., Holland, D., Rosing-Asvid, A., Yde, J. C., Liston, G. E., and Steffen, K.: Freshwater Flux and Spatiotemporal Simulated Runoff Variability into Ilulissat Icefjord, West Greenland, Linked to Salinity and Temperature Observations near Tidewater Glacier Margins Obtained Using Instrumented Ringed Seals, Journal of Physical Oceanography, https://doi.org/10.1175/JPO-D-14-0217.1, 2015.

Morlighem, M., Williams, C., Rignot, E., An, L., Arndt, J., Bamber, J., Catania, G., Chauché, N., Dowdeswell, J., Dorschel, B., Fenty, I., Hogan, K., Howat, I., Hubbard, A., Jakobsson, M., Jordan, T., Kjeldsen, K., Millan, R., Mayer, L., Mouginot, J., Noël, B., O'Cofaigh, C.,

https://doi.org/10.5194/egusphere-2025-1492
Preprint. Discussion started: 4 April 2025

Palmer, S., Rysgaard, S., Seroussi, H., Siegert, M., Slabon, P., Straneo, F., van den Broeke, M., Weinrebe, W., Wood, M., and Zinglersen, K.: IceBridge BedMachine Greenland. (IDBMG4, Version 5). [Data Set]., https://doi.org/10.5067/GMEVBWFLWA7X, 2022.

Motyka, R. J., Truffer, M., Fahnestock, M., Mortensen, J., Rysgaard, S., and Howat, I.: Submarine melting of the 1985 Jakobshavn Isbræ floating tongue and the triggering of the current retreat, Journal of Geophysical Research: Earth Surface, 116, https://doi.org/10.1029/2009JF001632, 2011.

Muench, R. D.: Oceanographic observations in Baffin Bay during July-September 1968, Washington, D.C. : Coast Guard, Oceanographic Unit, https://doi.org/10.5962/bhl.title.17035, 1971.

Muilwijk, M., Straneo, F., Slater, D. A., Smedsrud, L. H., Holte, J., Wood, M., Andresen, C. S., and Harden, B.: Export of Ice Sheet Meltwater from Upernavik Fjord, West Greenland, Journal of Physical Oceanography, 52, 363–382, https://doi.org/10.1175/JPO-D-21-0084.1, 2022.

Myers, P. G. and Ribergaard, M. H.: Warming of the Polar Water Layer in Disko Bay and Potential Impact on Jakobshavn Isbrae, Journal of Physical Oceanography, 43, 2629–2640, https://doi.org/10.1175/JPO-D-12-051.1, 2013.

Nielsen TG and Hansen B: Plankton community structure and carbon cycling on the western coast of Greenland during and after the sedimentation of a diatom bloom, Marine Ecology Progress Series, 125, 239–257, https://doi.org/10.3354/meps125239, 1995.

Oceans Melting Greenland: OMG Ocean Water Properties Data from Alamo Floats Version 1. Ver. 1., https://doi.org/10.5067/OMGEV-ALMO1, 2022.

Oliver, H., Slater, D., Carroll, D., Wood, M., Morlighem, M., and Hopwood, M. J.: Greenland Subglacial Discharge as a Driver of Hotspots of Increasing Coastal Chlorophyll Since the Early 2000s, Geophysical Research Letters, 50, https://doi.org/10.1029/2022GL102689, 2023.

Pacini, A., Pickart, R. S., Bahr, F., Torres, D. J., Ramsey, A. L., Holte, J., Karstensen, J., Oltmanns, M., Straneo, F., Bras, I. A. L., Moore, G. W. K., and Jong, M. F. d.: Mean Conditions and Seasonality of the West Greenland Boundary Current System near Cape Farewell, Journal of Physical Oceanography, https://doi.org/10.1175/JPO-D-20-0086.1, 2020.

Petersen, G.: The hydrography, primary production, bathymetry and "Tagsaq" of Disko Bugt, West Greenland, 159, 1–45, 1964.

Pickart, R. S., Torres, D. J., and Clarke, R. A.: Hydrography of the Labrador Sea during Active Convection, Journal of Physical Oceanography, https://doi.org/https://doi.org/10.1175/1520-0485(2002)032<0428:HOTLSD>2.0.CO;2, 2002.

Rysgaard, S., Boone, W., Carlson, D., Sejr, M. K., Bendtsen, J., Juul-Pedersen, T., Lund, H., Meire, L., and Mortensen, J.: An Updated View on Water Masses on the pan-West Greenland Continental Shelf and Their Link to Proglacial Fjords, Journal of Geophysical Research: Oceans, 125, e2019JC015 564, https://doi.org/10.1029/2019JC015564, 2020.

Scheick, J., Enderlin, E. M., and Hamilton, G.: Semi-automated open water iceberg detection from Landsat applied to Disko Bay, West Greenland, Journal of Glaciology, 65, 468–480, https://doi.org/10.1017/jog.2019.23, 2019.

Semper, S., Våge, K., Fer, I., Latuta, L., and Skjelsvik, S.: Formation and circulation of dense water from a two-year moored record in the northwestern Iceland Sea, Manuscript in review in Journal of Geophysical Research: Oceans, 2024.

Sloth, P. and Buch, E.: On the hydrography and watermass exchange of Disko Bay, ICES C.M. Doc. Tech. Rep. C:26, 17 pp, 1984.

Straneo, F. and Cenedese, C.: The Dynamics of Greenland's Glacial Fjords and Their Role in Climate, Annual Review of Marine Science, 7, 89–112, https://doi.org/10.1146/annurev-marine-010213-135133, 2015.

Straneo, F., Sutherland, D. A., Holland, D., Gladish, C., Hamilton, G. S., Johnson, H. L., Rignot, E., Xu, Y., and Koppes, M.: Characteristics of ocean waters reaching Greenland's glaciers, Annals of Glaciology, 53, 202–210, https://doi.org/10.3189/2012AoG60A059, 2012.

Wong, A., Keeley, R., and Carval, T.: Argo Quality Control Manual for CTD and Trajectory Data, https://doi.org/10.13155/33951, 2024.